CRYSTAL GROWTH & DESIGN

Article

Cite This: Cryst. Growth Des. 2019, 19, 5088−5096

pubs.acs.org/crystal

Crystalline GaAs Thin Film Growth on a c-Plane Sapphire Substrate

Samir K. Saha,[†] Rahul Kumar,[*,†] Andrian Kuchuk,[†] Mohammad Z. Alavijeh,[†] Yurii Maidaniuk,[†] Yuriy I. Mazur,[†] Shui-Qing Yu,[‡] and Gregory J. Salamo[†]

[†]Institute for Nanoscience and Engineering and [‡]Department of Electrical Engineering, University of Arkansas, Fayetteville, Arkansas 72701, United States

ABSTRACT: Crystalline zinc blende GaAs has been grown on a trigonal c-plane sapphire substrate by molecular beam epitaxy. The initial stage of GaAs thin film growth has been investigated extensively in this paper. When grown on c-plane sapphire, it takes (111) crystal orientation with twinning as a major problem. Direct growth of GaAs on sapphire results in three-dimensional GaAs islands, almost 50% twin volume, and a weak in-plane correlation with the substrate. Introducing a thin AlAs nucleation layer results in complete wetting of the substrate, better in-plane correlation with the substrate, and reduced twinning to 16%. Further, we investigated the effect of growth temperature, pregrowth sapphire substrate surface treatment, and in-situ annealing on the quality of the GaAs epilayer. We have been able to reduce the twin volume below 2% and an X-ray diffraction rocking curve line width to 223 arcsec. A good quality GaAs on sapphire can result in the implementation of microwave photonic functionality on a photonic chip.

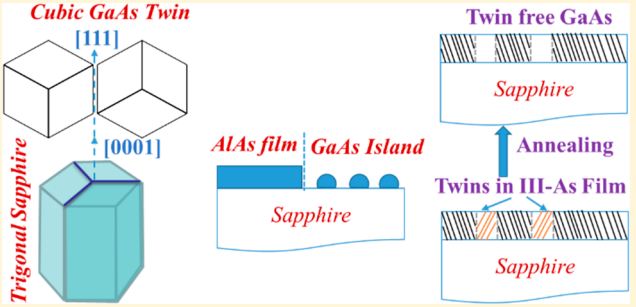

I. INTRODUCTION

Heteroepitaxy of III−V semiconductors is a well-established field. Generally, the heteroepitaxy term is used to denote the growth of different materials having a similar crystal structure but a different lattice constant, such as In(Ga)As on GaAs.[1,2] Very few examples exist in the literature regarding single-crystal epitaxy of two dissimilar crystal structures, such as cubic on wurtzite or cubic on trigonal. One successful effort has been the growth of crystalline cubic SiGe on a trigonal sapphire (Al_2O_3) substrate.[3,4] Likewise, there have been a few reports of thick GaAs film or GaAs nanostructures grown on sapphire.[5−10] Here, we report on the growth of a thin crystalline GaAs semiconductor on c-plane sapphire.

Our motivation to grow GaAs on sapphire is based on its potential use in III−V microwave photonics, optoelectronics, and electronics. This is based on important material properties, such as the large refractive index contrast between GaAs and sapphire, the high resistivity of the sapphire substrate, the transparency of the sapphire substrate near the III−As band gap, and importantly, the nearly equal thermal expansion coefficient of both materials. It is also based on the fact that III−V growth on Al_2O_3 (0001) can create the opportunity to realize monolithic integration, combining high-performance III−V semiconductor light sources, modulators and detectors, low loss waveguides and passive devices, and CMOS and RF silicon circuits on the same sapphire platform. The potential integration of microwave photonic (MWP) functionality and electronics on a single chip can dramatically increase the speed, bandwidth, processing capability, and dynamic range.

The challenge to realize these opportunities is the difficulty of epitaxial growth with such a very large disparity of lattice structure and large lattice mismatch (∼48%). It would seem that despite the exciting potential applications, this challenge has discouraged investigative research for the growth of these dissimilar materials. However, given that the sapphire substrate is expanding its territory in electronics and optoelectronics applications,[11] it is exciting and warranted to reexamine the possibility.

When GaAs is grown on c-plane sapphire, we may expect growth along the [111] direction since it is at least similar in lattice structure. Even in this case, however, the growth of GaAs (111) on sapphire is still a challenge because the lattice constant is dramatically different, which should lead to high surface roughness and defects related to stacking faults.[12] In addition to the large lattice mismatch and different crystal structure, we must also consider a third feature which is the chemical bonding at the interface between the two materials. For example, a high interfacial energy can lead to poor interaction between the two material surfaces. In this case, with a high lattice mismatch, different crystal structure, and unfavorable interface energy, one may expect poor crystal quality for GaAs on sapphire. On the other hand, GaAs may not even wet the sapphire substrate for a thin GaAs layer, and growth may occur by ignoring the high lattice mismatch and different crystal structure. In fact, this is more the case, as we observe the quality of GaAs (111) growth on c-plane sapphire to be high but with random twinning, which is the focus of this report.

Aligning the [111] cubic crystal direction to the [0001] hexagonal direction can have two possible azimuthal

Received: April 3, 2019
Revised: July 25, 2019
Published: August 2, 2019

DOI: 10.1021/acs.cgd.9b00448
Cryst. Growth Des. 2019, 19, 5088−5096

Table 1. Structural Details and Growth Parameters of Samples Presented in This Report

	AlAs nucleation layer (NL)		GaAs layer		
sample ID	growth temperature (°C)	thickness (nm)	growth temperature (°C)	thickness (nm)	substrate surface
C1	NA	NA	600	1	corrugated
C10	NA	NA	600	10	corrugated
C50	NA	NA	600	50	corrugated
S1	700	5	600	10	corrugated
S2	700	5	600	10	weak step-terrace
S3	700	5	600	10	step-terrace
T1	750	5	600	10	weak step-terrace
T2	750	5	550	10	weak step-terrace
T3	750	5	500	10	weak step-terrace
S50	700	5	600	50	corrugated
S50-annealed	700	5	600	50	corrugated

configurations.[3] These two phases will be rotated to each other by 60° and will be introduced during nucleation of GaAs on sapphire. Twins in GaAs (111) can also be introduced by insertion of a monolayer of wurtzite GaAs between two zinc blende GaAs regions rotated by 60° to each other.[13] Since twins can be introduced either during nucleation of III−As on sapphire or during further growth of material on already grown III−As, it is desirable to optimize the growth conditions throughout the growth of III−V material by carefully selecting nucleation layer material, growth parameter, substrate surface, etc.

To achieve this outcome, we have focused on the initial stage of growth of GaAs thin films on c-plane sapphire. More specifically, we have investigated the control of twinning for (a) direct growth of GaAs on c-plane sapphire; (b) growth of GaAs on sapphire but after an initial thin AlAs nucleation layer; (c) the effect of the pregrowth sapphire substrate surface treatment on GaAs growth, and (d) the role of the growth temperature and postgrowth in-situ annealing on GaAs growth on sapphire.

II. EXPERIMENTAL APPROACH

All the samples have been grown by solid source molecular beam epitaxy (MBE). Substrates were backside coated with 1 μm titanium for uniform and efficient heating. They were degreased with acetone, methanol, and deionized (DI) water and then immediately transferred to the load-lock chamber and heated at 200 °C for 1 h to mainly evaporate water vapor. Afterward, substrates were transferred to the degassing chamber where they were annealed at 850 °C for 6 h and then transferred to the growth chamber. In the growth chamber, substrates were heated to 900 °C for 3 h to get a clean smooth surface free of organic contaminants. Before starting the growth, we exposed the surface to an arsenic flux of 2×10^{-6} Torr at 650 °C for half an hour.[8] The substrate was then heated to the growth temperature according to the thermocouple reading. However, the actual surface temperature of the substrates may be 30−100 °C less than the thermocouple temperature since the thermocouple is not touching the surface of the substrates. The growth rate of GaAs and AlAs was 0.75 ML/s and 0.2 ML/s, respectively. The V/III flux ratio was 15. During the growth, real-time monitoring was done using reflection high energy electron diffraction (RHEED) set at 20 keV accelerating voltage and 1.5 A cathode current at a glancing angle of 1−2° to the substrate. Details of all samples grown are presented in Table 1, including the sapphire substrate preparation, growth temperature, and thicknesses of different layers.

The surface morphology of each sample was investigated by atomic force microscopy (AFM) (Bruker, model number 3000 dimension III) using the intermittent contact mode. AFM was performed using stable, sharp tips (Si tip material, tip radius ~10 nm) with optimized feedback and force parameters. To measure the optical properties, samples were mounted in a closed-cycle cryostat (Janis CCS-150) for the low-temperature photoluminescence (PL) measurements at 10 K. A 532 nm continuous-wave laser was used to excite the sample, and a liquid nitrogen cooled CCD detector array (Princeton Instruments PyLoN: 1024-1-7) attached to a 50 cm focal-length spectrometer (Acton 2500) was used to detect the photoluminescence (PL) signal. To understand the structural properties and crystalline quality of grown materials, a PANalytical X'Pert MRD diffractometer equipped with a multilayer focusing mirror, a standard four-bounce Ge (220) monochromator providing a collimated and monochromatic incident Cu Kα1 source of radiation (λ = 0.15406 nm), and a Pixel detector were used for the X-ray diffraction (XRD) scans.

III. RESULTS AND DISCUSSION

a. Direct Growth of GaAs/Sapphire. GaAs was grown directly on thermally clean c-plane sapphire. The RHEED pattern of the sapphire substrate before growth is shown in Figure 1a. Narrow streaks and Kikuchi lines indicate the high cleanliness and smoothness of the substrate surface. GaAs was grown at 600 °C, and three different samples corresponding to an amount of GaAs nominal thickness of 1 (C1), 10 (C10), and 50 nm (C50). These thickness values were calibrated for homoepitaxial GaAs growth. A spotty, but not a well-defined pattern, was observed by RHEED immediately as the growth started. Figure 1b shows the RHEED after GaAs growth. The spotty pattern indicates the 3D growth mode, whereas the presence of the ring pattern indicates the weak in-plane nature of the correlation of GaAs islands with the substrate. We observed that the GaAs islands were grown directly on the sapphire substrate without a wetting layer, thus indicating a type of Volmer−Weber (VW) growth mode. That is, because of the large lattice mismatch and high interfacial energy, the

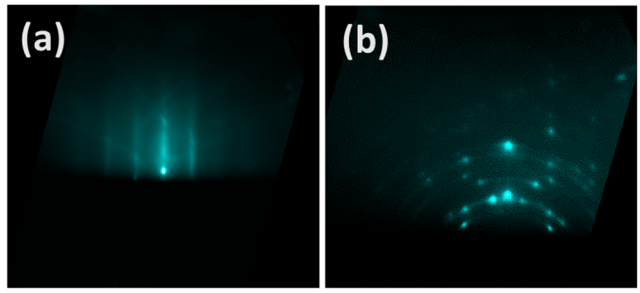

Figure 1. RHEED image (a) from thermally cleaned sapphire substrate (b) after 50 nm GaAs growth.

DOI: 10.1021/acs.cgd.9b00448
Cryst. Growth Des. 2019, 19, 5088−5096

structure becomes 3D islands as soon as the growth started with little attachment to the sapphire substrate. In fact, the GaAs 3D islands could be easily knocked off the surface with a light brush of the surface.

AFM images of all three samples show well-defined faceted GaAs nanocrystals as shown in Figure 2. As the GaAs

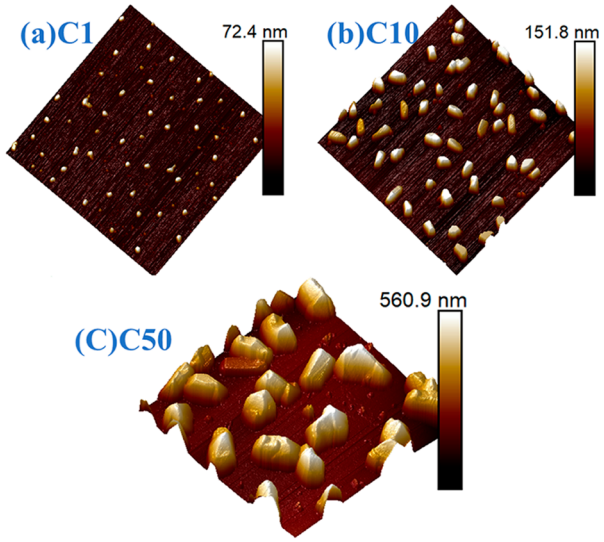

Figure 2. AFM images (5 μm × 5 μm) of samples (a) 1 nm GaAs, (b) 10 nm GaAs, (c) 50 nm GaAs.

deposition is increased, the island size is observed to increase while the density decreases. These values are listed in Table 2.

Table 2. GaAs Island Size, Density, and Percentage Surface Coverage with a Deposition Amount

GaAs nominal thickness (nm)	density (cm^{-2})	height (nm)	average lateral size (nm)	island coverage (%)
1	2E8	63.15	186.4	20
10	2.56E8	117.8	225	50
50	7.5E7	173	475	80

This can be explained by the coalescence and Ostwald ripening of islands due to the increased growth time. Facets of GaAs crystals can be observed in AFM images, illustrating the crystalline nature of islands.

By XRD ω-2θ scan, GaAs is found to be growing along the [111] direction with a small (220) peak, shown in Figure 3a. The fwhm of the rocking curves for the (111) plane versus the GaAs thickness is plotted in Figure 3b, and the lowest line width is observed for 50 nm GaAs which is 242 arcsec. The rocking curve (omega-scan) is a useful way to study the perfection of crystal planes when they are not parallel. Defects such as mosaicity, dislocations, and curvature create disruptions to the perfect parallelism of crystal planes. The low fwhm of rocking curve indicates the high quality of GaAs or very little deviation of GaAs islands from the [111] direction. Initial photoluminescence results (Figure 3c) from GaAs free exciton (FE) also support the high quality of the GaAs growth structure, with the lower energy peaks in PL likely due to defect states, possibly at the interface.

Asymmetric (220) phi-scan of GaAs shows a weak correlation with the sapphire substrate (as evident by broad 220 peaks) and a 6-fold symmetry instead of 3-fold, shown in Figure 4. We assign the observed 6-fold symmetry to the twin defects, i.e., two domains having the same out-of-plane orientation rotated by 60°. The interesting thing about these GaAs crystals is the excellent crystal quality and the random distribution of the two possible twin structures, probably because they are weakly correlated with the sapphire substrate. For example, very often during semiconductor/oxide growth, due to large lattice mismatch and interface energy, misfit dislocations at the interface are introduced as soon as critical nuclei form reducing the stress below a threading dislocation level so that growth can take place at its bulk lattice at low levels of strain.[14] The weak interfacial correlation of GaAs with the sapphire substrate could be the result of the formation of a large number of misfit dislocation at the interface. Since dislocations are limited to the semiconductor/oxide interface and do not propagate into the bulk of semiconductor, the result can be high-quality GaAs islands as shown by XRD images (Figure 3b). Apparently, sapphire is basically acting as a compliant substrate in these early investigations based the lattice mismatch and the weak chemical interaction.

b. Introduction of Thin AlAs Nucleation Layer. In spite of excellent crystallinity of the 3D islands, direct growth of GaAs on sapphire resulted in about 50% twin formation, weak interfacial correlation, and more than one out-of-plane crystal orientation. To improve on these structural shortcomings, we

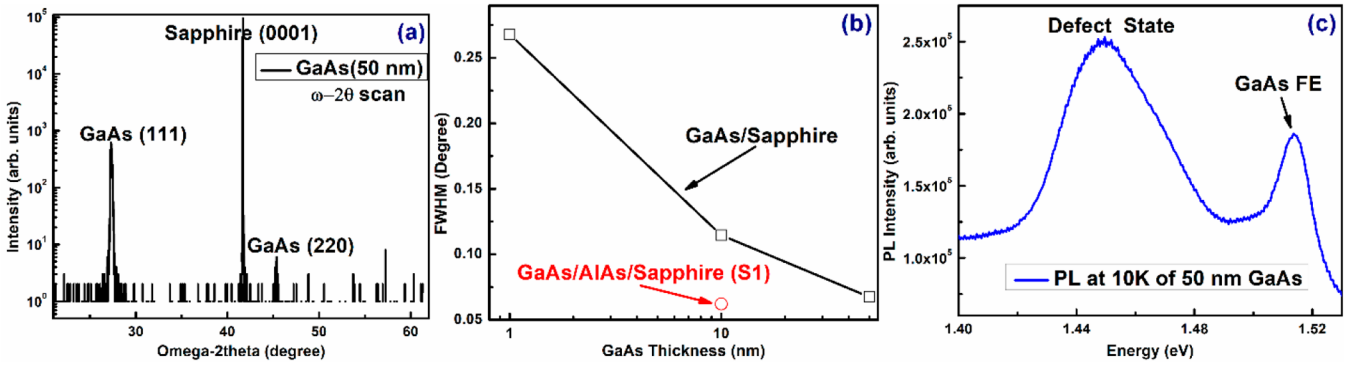

Figure 3. (a) ω-2θ scan of 50 nm GaAs, (b) change in fwhm of (111) rocking curve with GaAs deposition amount, (c) low-temperature PL from 50 nm GaAs (C50). This indicated improved crystal quality with increased growth and using an AlAs 5 nm nucleation layer (in red) discussed below.

DOI: 10.1021/acs.cgd.9b00448
Cryst. Growth Des. 2019, 19, 5088−5096

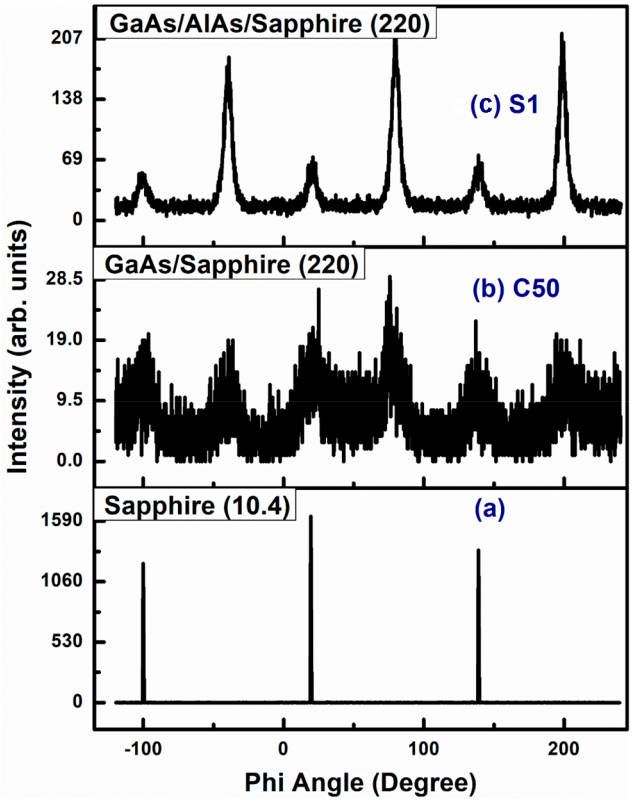

Figure 4. Phi-scan of (a) (10.4) plane of sapphire and (b) (220) plane of GaAs/sapphire (C50) and (c) GaAs/AlAs/sapphire (S1). This indicates reduced twining with an AlAs 5 nm nucleation layer.

introduced a thin (5 nm) AlAs deposition as a nucleation layer between the sapphire substrate and GaAs. One of the reasons to choose AlAs is the negligible lattice mismatch between GaAs and AlAs. RHEED from AlAs and from 10 nm GaAs grown on AlAs/sapphire is shown in Figure 5, panels a and b, respectively. A spotty pattern appeared with the gradual disappearance of streaks from the substrate just after the

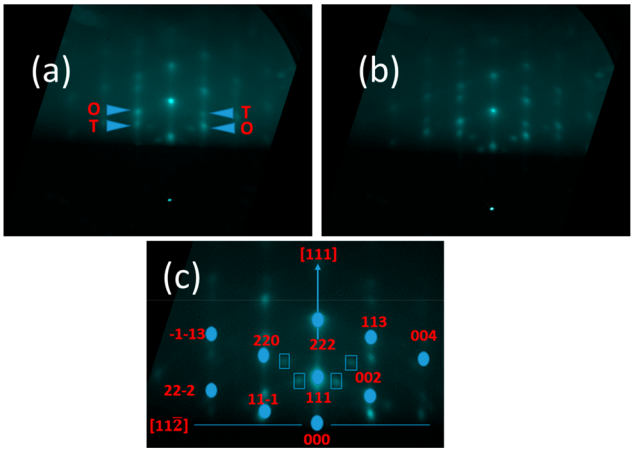

Figure 5. RHEED from sample S1 during (a) AlAs growth, (b) GaAs growth on sapphire ("O" refers to original phase, whereas "T" refers to twin phase), and (c) notation of planes for all RHEED spots for GaAs (111) growth. Both (a) and (b) RHEED patterns indicate twining. RHEED spots in the rectangle do not belong to GaAs (111) orientation.

growth started. These spots are located at a different location than the streak from the sapphire substrate indicating an abrupt *d*-spacing change and hence instant in-plane relaxation of AlAs. A closer look at the RHEED tells the superposition of two spotty patterns of different intensity. RHEED shows twin spots for a single plane, indicating the formation of one original preferential phase with a suppressed twin phase (original phase is denoted as "O" and twin phase is denoted as "T" in Figure 5a). AFM images of these structures are shown in Figure 6, depending on the starting substrate. A smooth surface is observed for sample S1, shown in Figure 6 (row (II) column (a)). AlAs is observed to wet the sapphire surface better than GaAs directly, possibly because of a higher bond strength between Al−O. Bond strength for Ga−O, As−O, and Al−O are 374, 484, and 502 kJ/mol, respectively.[15]

For the AlAs/GaAs/sapphire structures, only one out-of-plane crystal orientation [111] has been detected by a gonio-scan unlike the direct GaAs growth on sapphire. Although RHEED showed spots corresponding to the (111) orientation with its twin phase and some other orientation (probably (220) orientation), which is marked by a rectangle in Figure 5c, during growth of AlAs and GaAs. Volume of GaAs (220) orientation is not significant enough to be detected by XRD. The rocking curve fwhm of this structure is as low as 220 arcsec (shown in Figure 3b). Meanwhile, a phi-scan (Figure 4) shows the reduction of the twin volume to 16%, and sharp (220) peaks in the phi-scan indicate better in-plane correlation with the sapphire substrate compared to the direct growth of GaAs/sapphire. Twin reduction after AlAs nucleation layer could be related to the wetting and coalescence of AlAs islands. In the case of direct growth of GaAs on sapphire, individual islands can have either of the twin phases with equal probability, assuming there is no preference for either phase. Hence, we see no preference of any of these two phases when GaAs is grown directly on a sapphire substrate. In the case of AlAs nucleation layer, small AlAs islands coalesce and wet the substrate surface at the early stage of growth. During coalescence of 3D islands, one type of twin can expand at the expense of the other twin phase. This is consistent with the case of SiGe growth on sapphire, where formation of microtwin lamellas and a significant reduction of twin volume have been reported for a thick continuous SiGe layer after island coalescence[16] and explained by successive glides of the Shockley partial dislocations (surrounding each twin region) on the adjacent glide planes.[17,18] Together, these results show that introducing a thin layer of AlAs improves the wetting of the substrate, twinning, in-plane-correlation and results in better overall quality of GaAs. It should be noted here that improvement due to the AlAs nucleation layer is due to better chemical interaction between the AlAs and sapphire substrate than the GaAs and sapphire substrate.

c. Effect of Pregrowth Substrate Surface Treatment. Our investigation indicates that preparation of the sapphire substrate surface plays a key role in determining the GaAs film quality. This is in agreement with previous reports that the sapphire wafer treatment before deposition of an epilayer has been effective in reducing twinning.[19] More specifically surfaces with clear step-terraces have generally been effective in encouraging a layer-by-layer growth mode and is widely used to control both the quality and orientation of epilayer in heteroepitaxy.[20,21] To explore the role of the sapphire substrate surface on III−V growth, we investigated three different kinds of initial substrate surfaces: (a) a corrugated substrate surface

DOI: 10.1021/acs.cgd.9b00448
Cryst. Growth Des. 2019, 19, 5088−5096

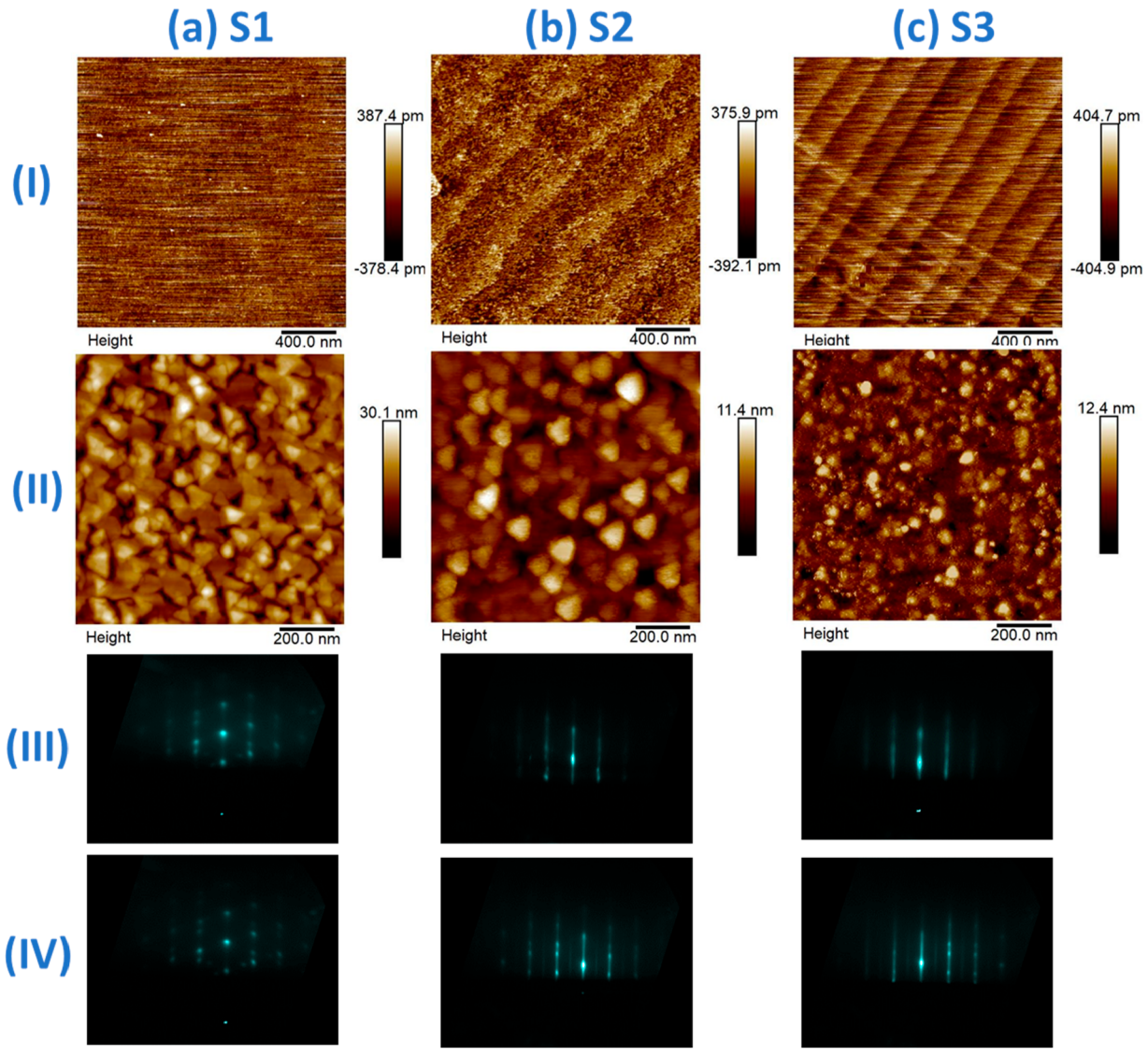

Figure 6. Columns show the data for (a) corrugated surface sample, (b) weakly defined step-terrace surface sample, and (c) well-defined step-terrace surface sample. Row (I) is an AFM image of the initial sapphire substrate, Row (II) is an AFM images of the GaAs film, Row (III) is the RHEED pattern after AlAs growth, while row (IV) is the RHEED pattern after GaAs growth. Both (a) and (b) RHEED patterns indicate twining, while the RHEED pattern in (c) indicates twining is absent only for AlAs (row III) growth.

with no step-terrace structure (S1); (b) a weakly defined step-terrace surface (S2); and (c) a well-defined step-terrace surface (S3). AFM images of these surfaces are shown in Figure 6. The initial 5 nm of the AlAs nucleation layer followed by 10 nm GaAs film was grown on all three substrates under the same growth conditions. In all three cases, we observed the wetting of the substrate. Of the three samples, GaAs grown on the well-defined step-terrace surface showed the best surface smoothness. For example, RHEED is streakier for the well-defined step-terrace surface, and reconstruction streaks can be seen from the GaAs during growth on the step-terrace surface. It is well-known that surface reconstruction changes with temperature for GaAs (111)B growth, while it remains invariant with growth temperature during GaAs (111)A growth.[22] A (2 × 2) surface reconstruction is observed, which remained invariant with substrate temperature variation similar to what is observed for homoepitaxial GaAs (111)A growth where only (2 × 2) surface reconstruction is observed.[23] Hence, orientation of the GaAs layer is (111)A in our grown samples.

Figure 7a shows the phi-scan of the GaAs (220) plane for all three samples grown on the different substrate surfaces. The twin volume for all the samples is the same. This demonstrates that the initial substrate surface has very little impact on twinning. However, in the case of a well-defined step-terrace surface, the (220) peak is sharper than the other two. This is due to a stronger in-plane correlation of the film with the sapphire substrate. Complementing this result, Figure 7b shows the omega-2theta scan for the three samples, indicating that the surface with step-terraces has fringes in the omega-2theta scan. This indicates higher-quality heterointerfaces. Rocking curves show that the intensity dispersion at the base is largest for GaAs on corrugated surface and least for GaAs on a well-defined step-terrace surface. These rocking curves could be well fitted with two Gaussian curves: one having smaller intensity and larger line width, while the second having a larger

DOI: 10.1021/acs.cgd.9b00448
Cryst. Growth Des. 2019, 19, 5088−5096

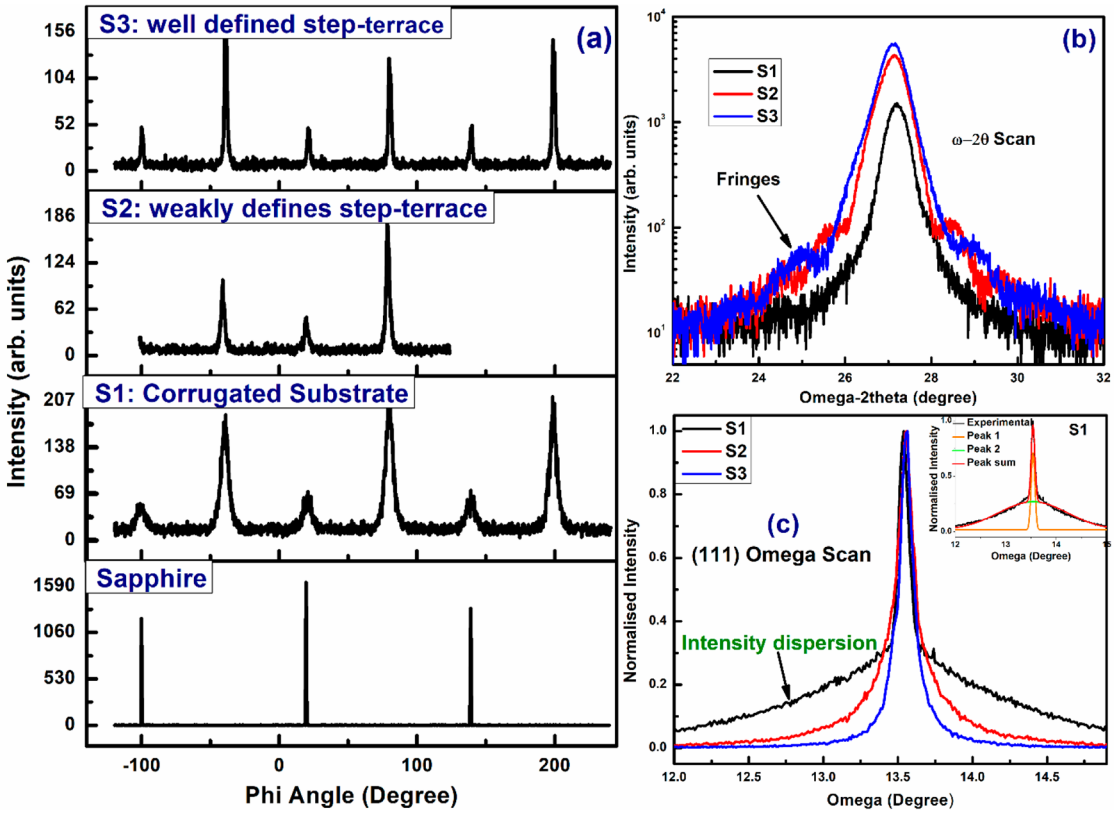

Figure 7. (a) Phi-scan, (b) (111) omega-2theta scan, and (c) (111) omega-scan of samples grown on the different starting substrate surfaces. Inset in the Figure 7c shows the Gaussian fitting of omega-scan of S1 into two peaks having different broadness.

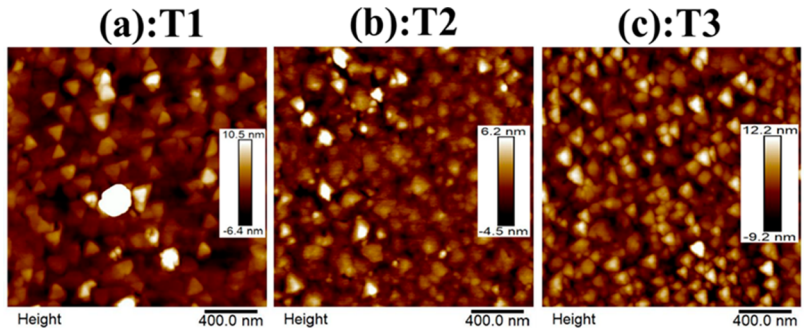

Figure 8. AFM images of GaAs samples grown at three different growth temperatures (a) 600 °C (T1), (b) 550 °C (T2), and (c) 500 °C (T3).

intensity and smaller line width (shown in inset of Figure 7c for sample S1). One likely explanation for this behavior is that the two peaks come from two different materials with the broader peak originating from the AlAs nucleation layer (which is very thin giving a broad peak) and a sharp peak from the thicker GaAs layer. This is difficult to test, but the fitting consistently shows a small shift for the broader peak toward a larger lattice constant. Better in-plane correlation with the substrate and higher-quality heterointerface formation in the case of step-terrace surfaces can be explained by nucleation via a stronger interaction with the substrate at the step edges.

d. Effect of Growth Temperature. The growth of high-quality epitaxial layers can be expected to be dependent on a number of factors such as growth temperatures,[24] the ratio of V/III beam fluxes, growth rate, a high quality, and atomically flat substrate. This is supported by early reports of homoepitaxial growth of GaAs (111)[12,13,24] indicating that the morphology and overall epilayer quality are very sensitive to such growth parameters, especially temperature. To investigate the effect of growth temperature on the GaAs film quality, surface morphology, and film−substrate correlation, GaAs was grown at three different growth temperatures, namely, 600 °C (T1), 550 °C (T2), and 500 °C (T3). Surface morphologies of these samples are shown in Figure 8. The root-mean-square roughness (RMS) of these samples grown at 600 °C, 550 °C, and 500 °C are 4.59, 1.7, and 3.72 nm, respectively. Pyramidal shape hillocks can be seen on these surfaces and is characteristic of GaAs (111) growth.[22,25,26] For samples grown at 550 °C, the surface is smoother as very few pyramidal hillocks are present in this sample compared to the other two samples.

Phi-scans of these samples (Figure 9a) showed that the growth temperature affects twinning considerably. Samples grown at a relatively low temperature (500 °C) show the

DOI: 10.1021/acs.cgd.9b00448
Cryst. Growth Des. 2019, 19, 5088−5096

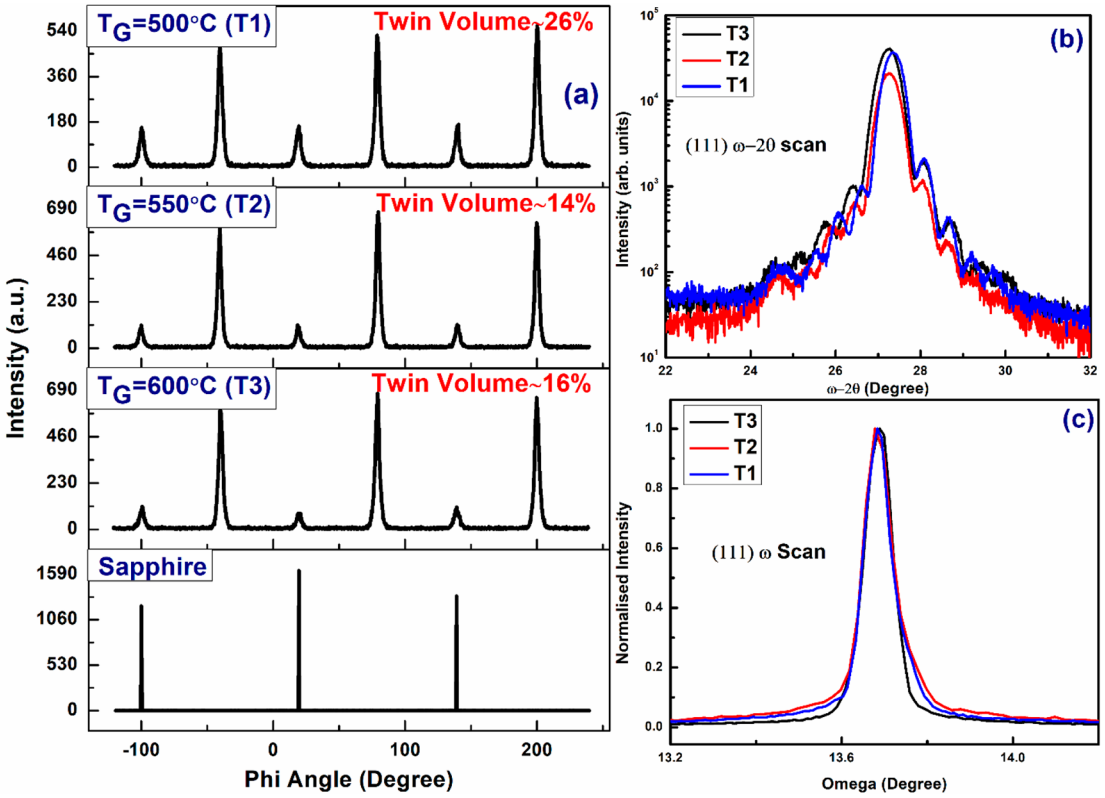

Figure 9. (a) (220) phi-scan, (b) (111) omega-2theta scan, and (c) (111) omega-scan of samples grown on different growth temperatures.

highest twin volume. The symmetric omega-2theta scan in Figure 9b indicates only the (111) crystal orientation. Fringes can be observed in all three samples indicating an abrupt heterointerface formation. The fringe spacing decreases with the temperature indicating that the thickness of the GaAs layer is certainly dependent on the growth temperature. However, GaAs rocking curves around the [111] direction (Figure 9c) show that samples have almost the same fwhm, which indicates that the (111) plane deviation from its mean position is the same in all three samples.

e. Effect of In-Situ Annealing. Our investigation on annealing our samples indicated that annealing can be used to improve both the surface and the bulk of the grown film.[27] In this work, we performed in-situ annealing of GaAs (50 nm) grown on AlAs/Sapphire under As_2 overpressure to investigate its effect on surface and bulk properties of GaAs. In-situ annealing improved the GaAs crystal quality by reducing the twinning ratio by removing one of the twin domains. Figure 10a,b shows the RHEED pattern after growth of 50 nm of GaAs on the AlAs/sapphire (S50) and in-situ annealed under arsenic overpressure at 800 °C for 1 min, respectively. The RHEED changed from the spotty pattern to streaky-spotty pattern with no observable twinning. Reconstruction streaks indicate a good quality smooth surface. The AFM image of S50, shown in Figure 10c, shows the characteristic pyramidal features. AFM images of the same in-situ annealed 50 nm GaAs sample (S50-annealed) are shown in Figure 10d,e. The in-situ annealed sample shows the appearance of surface pits with an otherwise smooth surface. Spots in the RHEED for this surface are due to the surface pits.

Two different types of pits can be observed in the AFM images of S50-annealed sample: triangular pits (which is small in size) and irregular-shaped pits (big in size). Edges of the triangles are aligned in particular in-plane directions. Larger, irregular-shaped pits could be the result of agglomeration of multiple triangular shaped pits or expansion of these triangular pits laterally due to desorption. This is consistent with previous studies on GaAs (111)A growth, where triangular base stacking faults are observed and grow into 3D stacking fault tetrahedrons (SFT).[28] These SFTs are the region of the twin volume. They are apparently thermodynamically unstable possibly due to their small size and defect boundary. As a result, at the annealing temperature, the triangular pits can form due to the evaporation (or desorption) of material from the SFTs. Supporting this explanation, the surface area of the pits is a similar fraction of the total surface area, indicating that the minor twin has evaporated leaving only original phase behind.

A phi-scan of the in-situ annealed sample (Figure 11) shows the twin volume is now less than 2%. This is consistent with our explanation that the triangular shape of the stacking faults can be the reason for the formation of triangular pits.

Given that the material from SFTs evaporates during annealing, and the in-situ annealed sample shows only one phase remaining, optimization of the annealing temperature and time can result in a twin-free GaAs layer. This can be used as an initial template for high-quality GaAs growth for electronic and optoelectronics applications. Further studies will focus on optimizing growth and annealing parameters for obtaining twin-free GaAs template for device-quality GaAs growth.

IV. CONCLUSION

A highly dissimilar material system of GaAs on c-plane sapphire has been grown. For direct growth of GaAs on c-plane sapphire, we observed that growth proceeds in a 3D growth

DOI: 10.1021/acs.cgd.9b00448
Cryst. Growth Des. 2019, 19, 5088−5096

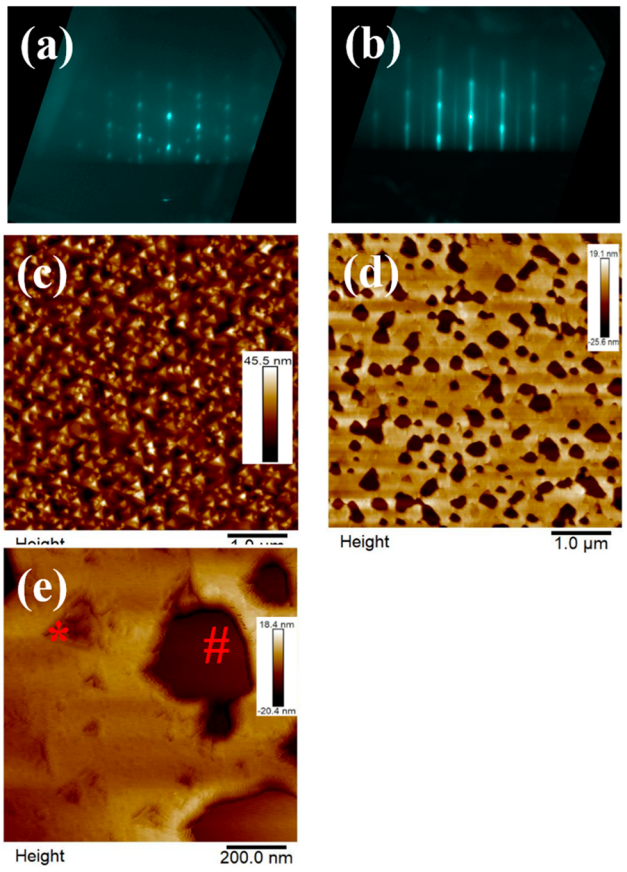

Figure 10. RHEED pattern from sample A1 (a) after the GaAs growth and (b) after in-situ annealing; 5 μm × 5 μm AFM image of (c) 50 nm GaAs (S50), (d) after in-situ annealed sample (S50-annealed) (e) 1 μm × 1 μm AFM images of the in-situ annealed sample. Symbol "*" shows a triangular pit, whereas symbol "#" shows an irregular-shaped pit.

mode with very poor wetting of the surface, comparatively weak substrate to film interaction, and the formation of twin structures. Surface wetting was improved by introducing a thin AlAs layer which acted as a nucleation layer between the sapphire substrate and the GaAs film. Higher wetting and improved in-plane correlation with the substrate is explained by the higher bond strength of Al−O. The observed twin ratio reduction is likely correlated to the coalescence of small AlAs 3D islands. To uncover control of twining, we investigated the role of the starting substrate on nucleation by examining the pregrowth substrate treatment on the GaAs growth. We found improved heterointerface formation and better surface morphology in the case of well-defined step-terrace substrate surface. Likewise, we also found that the twin formation and GaAs surface morphology was very sensitive on the growth temperature and in-situ annealing. In-situ annealing was very effective to reduce the twinning. Our in-situ annealed GaAs film showed that the twin volume is less than 2%. Apparently annealing reduced twinning by removing one of the twin domains leaving scars in the form of triangle holes but was otherwise smooth. This gives us confidence that further optimization of growth parameters and annealing parameters (annealing time and temperature) can result in an even smoother and twin-free GaAs film demonstrating the quality growth of dissimilar materials.

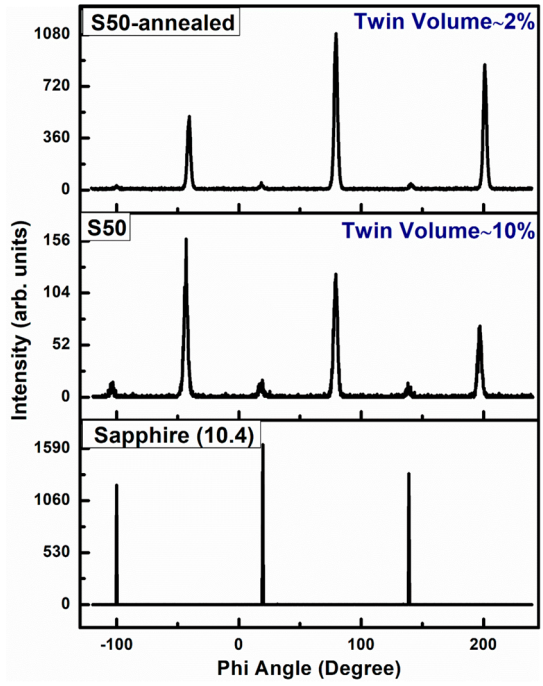

Figure 11. Phi-scan of (10.4) plane of sapphire and (220) plane of 50 nm GaAs sample (S50) and in-situ annealed sample (S50-annealed).

AUTHOR INFORMATION

Corresponding Author

*E-mail: rkp203@gmail.com.

ORCID

Rahul Kumar: 0000-0003-4093-6180

Andrian Kuchuk: 0000-0002-0571-6169

Yuriy I. Mazur: 0000-0002-0884-6049

Notes

The authors declare no competing financial interest.

ACKNOWLEDGMENTS

The authors acknowledge the financial support by the Institute of Nanoscale Science and Engineering, University of Arkansas, and the Project "Quantum Interfaces of Dissimilar Materials" funded by National Science Foundation (NSF) (Grant No. 1809054).

REFERENCES

(1) Kumar, R.; Bag, A.; Mukhopadhyay, P.; Das, S.; Biswas, D. Comparison of Different Grading Schemes in InGaAs Metamorphic Buffers on GaAs Substrate: Tilt Dependence on Cross-Hatch Irregularities. *Appl. Surf. Sci.* **2015**, *357*, 922−930.

(2) Kumar, R.; Maidaniuk, Y.; Kuchuk, A.; Saha, S. K.; Ghosh, P. K.; Mazur, Y. I.; Ware, M. E.; Salamo, G. J. Excitation Intensity and Thickness Dependent Emission Mechanism from an Ultrathin InAs Layer in GaAs Matrix. *J. Appl. Phys.* **2018**, *124* (23), 235303.

(3) Park, Y.; King, G. C.; Choi, S. H. Rhombohedral Epitaxy of Cubic SiGe on Trigonal c-Plane Sapphire. *J. Cryst. Growth* **2008**, *310* (11), 2724−2731.

(4) Kim, H. J.; Duzik, A.; Choi, S. H. Lattice-Alignment Mechanism of SiGe on Sapphire. *Acta Mater.* **2018**, *145*, 1−7.

(5) Sugimura, A.; Hosoi, T.; Ishibitsu, K.; Kawamura, T. Heteroepitaxial Growth of GaAs on Sapphire Substrates by a Three-Step Method Using Low Pressure MOCVD. *J. Cryst. Growth* **1986**, *77* (1−3), 524−529.

DOI: 10.1021/acs.cgd.9b00448
Cryst. Growth Des. 2019, 19, 5088−5096

(6) Kasai, K.; Nakai, K.; Ozeki, M. Material and Device Properties of GaAs on Sapphire Grown by Metalorganic Chemical Vapor Deposition. *J. Appl. Phys.* **1986**, *60* (1), 1−5.
(7) Humphreys, T. P.; Miner, C. J.; Posthill, J. B.; Das, K.; Summerville, M. K.; Nemanich, R. J.; Sukow, C. A.; Parikh, N. R. Heteroepitaxial Growth and Characterization of GaAs on Silicon-on-sapphire and Sapphire Substrates. *Appl. Phys. Lett.* **1989**, *54* (17), 1687−1689.
(8) Humphreys, T. P.; Miner, C. J.; Parikh, N. R.; Das, K.; Summerville, M. K.; Posthill, J. B.; Nemanich, R. J.; Sukow, C. A. Molecular Beam Epitaxial Growth and Characterization of GaAs on Sapphire and Silicon-on-Sapphire Substrates. *MRS Proc.* **1988**, *144*, 195.
(9) Kuech, T. F.; Segmüller, A.; Kuan, T. S.; Goorsky, M. S. Growth and Properties of Thin GaAs Epitaxial Layers on Al 2 O 3. *J. Appl. Phys.* **1990**, *67* (10), 6497−6506.
(10) Chuang, L. C.; Moewe, M.; Ng, K. W.; Tran, T.-T. D.; Crankshaw, S.; Chen, R.; Ko, W. S.; Chang-Hasnain, C. GaAs Nanoneedles Grown on Sapphire. *Appl. Phys. Lett.* **2011**, *98* (12), 123101.
(11) Nakasu, T.; Kizu, T.; Yamashita, S.; Aiba, T.; Hattori, S.; Sun, W.-C.; Taguri, K.; Kazami, F.; Hashimoto, Y.; Ozaki, S.; et al. Surface Texture and Crystallinity Variation of ZnTe Epilayers Grown on the Step-Terrace Structure of the Sapphire Substrate. *J. Electron. Mater.* **2016**, *45* (4), 2127−2132.
(12) Esposito, L.; Bietti, S.; Fedorov, A.; Nötzel, R.; Sanguinetti, S. Ehrlich-Schwöbel Effect on the Growth Dynamics of GaAs(111)A Surfaces. *Phys. Rev. Mater.* **2017**, *1* (2), 24602.
(13) Park, Y.; Cich, M. J.; Zhao, R.; Specht, P.; Weber, E. R.; Stach, E.; Nozaki, S. Analysis of Twin Defects in GaAs(111)B Molecular Beam Epitaxy Growth. *J. Vac. Sci. Technol., B: Microelectron. Process. Phenom.* **2000**, *18* (3), 1566.
(14) Saint-Girons, G.; Cheng, J.; Regreny, P.; Largeau, L.; Patriarche, G.; Hollinger, G. Accommodation at the Interface of Highly Dissimilar Semiconductor/oxide Epitaxial Systems. *Phys. Rev. B: Condens. Matter Mater. Phys.* **2009**, *80* (15), 155308.
(15) Luo, Y.-R.; Luo, Y.-R. *Comprehensive Handbook of Chemical Bond Energies*; CRC Press, 2007.
(16) Kim, H.-J.; Bae, H.-B.; Park, Y.; Lee, K.; Choi, S. H. Temperature Dependence of Crystalline SiGe Growth on Sapphire (0001) Substrates by Sputtering. *J. Cryst. Growth* **2012**, *353* (1), 124−128.
(17) Wegscheider, W.; Eberl, K.; Abstreiter, G.; Cerva, H.; Oppolzer, H. Novel Relaxation Process in Strained Si/Ge Superlattices Grown on Ge (001). *Appl. Phys. Lett.* **1990**, *57* (15), 1496−1498.
(18) Wegscheider, W.; Cerva, H. Effect of Compressive and Tensile Strain on Misfit Dislocation Injection in SiGe Epitaxial Layers. *J. Vac. Sci. Technol., B: Microelectron. Process. Phenom.* **1993**, *11* (3), 1056.
(19) Kim, H. J.; Park, Y.; Bae, H. B.; Choi, S. H. High-Electron-Mobility SiGe on Sapphire Substrate for Fast Chipsets. *Adv. Condens. Matter Phys.* **2015**, *2015*, 1−9.
(20) Yanagiya, S.; Kamimura, S.; Fujii, M.; Ishida, M.; Moriyasu, Y.; Matsui, M.; Yoshimoto, M.; Ohnishi, T.; Yoshida, K.; Sasaki, K.; et al. Self-Formed Silicon Quantum Wires on Ultrasmooth Sapphire Substrates. *Appl. Phys. Lett.* **1997**, *71* (10), 1409.
(21) Maeda, T.; Yoshimoto, M.; Ohnishi, T.; Lee, G. H.; Koinuma, H. Orientation-Defined Molecular Layer Epitaxy of α-Al2O3 Thin Films. *J. Cryst. Growth* **1997**, *177* (1−2), 95−101.
(22) Woolf, D. A.; Westwood, D. I.; Williams, R. H. The Homoepitaxial Growth of GaAs(111)A and (111)B by Molecular Beam Epitaxy: An Investigation of the Temperature-Dependent Surface Reconstructions and Bulk Electrical Conductivity Transitions. *Semicond. Sci. Technol.* **1993**, *8* (6), 1075−1081.
(23) Woolf, D. A.; Westwood, D. I.; Williams, R. H. The Homoepitaxial Growth of GaAs(111)A and (111)B by Molecular Beam Epitaxy: An Investigation of the Temperature-Dependent Surface Reconstructions and Bulk Electrical Conductivity Transitions. *Semicond. Sci. Technol.* **1993**, *8* (6), 1075−1081.
(24) Sato, K.; Fahy, M. R.; Joyce, B. A. The Growth of High Quality GaAs on GaAs (111)A. *Jpn. J. Appl. Phys.* **1994**, *33*, L905−L907.
(25) Sato, K.; Fahy, M. R.; Joyce, B. A. The Growth of High Quality GaAs on GaAs (111)A. *Jpn. J. Appl. Phys.* **1994**, *33*, L905−L907.
(26) Horikoshi, Y.; Uehara, T.; Iwai, T.; Yoshiba, I. Area Selective Growth of GaAs by Migration-Enhanced Epitaxy. *Phys. Status Solidi B* **2007**, *244* (8), 2697−2706.
(27) Yamaguchi, M.; Tachikawa, M.; Itoh, Y.; Sugo, M.; Kondo, S. Thermal Annealing Effects of Defect Reduction in GaAs on Si Substrates. *J. Appl. Phys.* **1990**, *68* (9), 4518−4522.
(28) Uehara, T.; Iwai, T.; Yoshiba, I.; Horikoshi, Y. Area-Selective Epitaxial Growth of GaAs on GaAs(111)A Substrates by Migration-Enhanced Epitaxy. *Jpn. J. Appl. Phys.* **2007**, *46* (2), 496−501.

DOI: 10.1021/acs.cgd.9b00448
Cryst. Growth Des. 2019, 19, 5088−5096